


Proceeding Paper

Simulation of Indirect ^{13}C – ^{13}C J -Coupling Tensors in Diamond Clusters Hosting the NV Center [†]

Alexander Nizovtsev ^{1,2,*}, Aliaksandr Pushkarchuk ^{2,3}, Semen Kuten ⁴, Dominik Michels ⁵, Dmitry Lyakhov ⁵, Nikolai Kargin ² and Sergei Kilin ¹ 

¹ Institute of Physics, National Academy of Science, 220072 Minsk, Belarus; sergei_kilin@yahoo.com

² National Research Nuclear University “MEPhI”, Moscow 115409, Russia; alexp51@bk.ru (A.P.); nikargin@mephi.ru (N.K.)

³ Institute of Physical and Organic Chemistry, National Academy of Science, 220072 Minsk, Belarus

⁴ Institute for Nuclear Problems, Belarusian State University, 220006 Minsk, Belarus; semen_kuten@list.ru

⁵ Computer, Electrical and Mathematical Science and Engineering Division, 4700 King Abdullah University of Science and Technology (KAUST), Thuwal 23955-6900, Saudi Arabia; dominik.michels@kaust.edu.sa (D.M.); dmitry.lyakhov@kaust.edu.sa (D.L.)

* Correspondence: apniz@dragon.bas-net.by

[†] Presented at the 3rd International Online-Conference on Nanomaterials, 25 April–10 May 2022; Available online: <https://iocn2022.sciforum.net/>.

Abstract: The full tensors ${}^nJ_{KL}$ ($K, L = X, Y, Z$), describing n -bond J -coupling of nuclear spins ^{13}C in H-terminated diamond-like clusters $\text{C}_{10}\text{H}_{16}$ (adamantane) and $\text{C}_{35}\text{H}_{36}$, as well as in the cluster $\text{C}_{33}[\text{NV}^-]\text{H}_{36}$ hosting the negatively charged NV^- center, were simulated. We found that, in addition to the usually considered isotropic scalar nJ -coupling constant, the anisotropic contributions to the nJ -coupling tensor are essential. We also showed that the presence of the NV center affects the J -coupling characteristics, especially in the case of ^{13}C – ^{13}C pairs located near the vacancy of the NV center.

Keywords: solid-state NMR; $J_{\text{C-C}}$ -coupling tensor; H-terminated diamond cluster; NV center; DFT simulation



Citation: Nizovtsev, A.; Pushkarchuk, A.; Kuten, S.; Michels, D.; Lyakhov, D.; Kargin, N.; Kilin, S. Simulation of Indirect ^{13}C – ^{13}C J -Coupling Tensors in Diamond Clusters Hosting the NV Center. *Mater. Proc.* **2022**, *9*, 4. <https://doi.org/10.3390/materproc2022009004>

Academic Editor: Antonio Di Bartolomeo

Published: 22 April 2022

Publisher’s Note: MDPI stays neutral with regard to jurisdictional claims in published maps and institutional affiliations.



Copyright: © 2022 by the authors. Licensee MDPI, Basel, Switzerland. This article is an open access article distributed under the terms and conditions of the Creative Commons Attribution (CC BY) license (<https://creativecommons.org/licenses/by/4.0/>).

1. Introduction

In the past decade, there was rapid progress in the development of quantum magnetic sensing technologies based on nitrogen-vacancy (NV) color centers in diamond (e.g., see [1,2] for recent reviews). A magnetometer based on a single NV center can have nanometer-scale spatial resolution and exceptional sensitivity (up to ~Hz) allowing the detection of target single ^{13}C nuclear spins or coupled ^{13}C – ^{13}C pairs located within the diamond, which can be used as long-lived quantum memory [3]. Moreover, an NV-based magnetometer allows to distinguish (by chemical shifts) inequivalent nuclear spins of molecules located at diamond surface [4]. This enables a new exciting application area of single-spin nuclear magnetic resonance (NMR) to investigate important issues ranging from determination of molecular structures of inorganic/biological compounds up to medical imaging for therapeutic matters. In these respects, predicting high-resolution NMR characteristics for studied spin systems is essential. Among them, the characteristics of indirect nuclear spin–spin coupling (J -coupling) that arise due to second-order hyperfine interactions with electrons from chemical bonds connecting nuclei are important. Generally, a second-rank tensor ${}^nJ_{KL}$ ($K, L = X, Y, Z$) is required to fully describe J -coupling between two nuclei [5]. However, until recently, most high-resolution NMR experiments were focused on measuring only isotropic scalar constant ${}^nJ_{iso} = \text{Sp}^nJ_{KL}/3$ because the anisotropic parts of the J -tensor were averaged out to zero by fast molecular motion in solution-state NMR or fast magic-angle spinning (MAS) in solid-state experiments [6–8]. Meanwhile, in the case of crystalline solids, the constituent atoms are located in a certain order determined by

the crystal structure so that many important NMR interactions are orientation dependent and the information about anisotropic NMR interaction tensors becomes essential [5,8]. In particular, both the symmetric $^1J_{iso} = (^1J_{ZZ} + ^1J_{XX} + ^1J_{YY})/3$ (≈ 70 Hz) and the asymmetric $\Delta^1J = ^1J_{ZZ} - (^1J_{XX} + ^1J_{YY})/2$ (≈ 90 Hz) parts of the J -coupling tensor $^1J_{KL}$ for the nearest-neighbor (N–N) ^{29}Si nuclear spins have been recently determined in single-crystal silicon [9]. This was achieved by measuring the NMR lineshapes which are sensitive to the value of Δ^1J , at four different crystallographic orientations relative to the applied magnetic field. In diamond with ^{13}C nuclear spins, which is of the main interest here, an analogous experiment was undertaken many years ago [10] but no J -coupling effects were studied there due to low sensitivity. In addition, as far as we know, there were no theoretical works on the quantum-chemical calculation of the J -coupling characteristics of ^{13}C nuclear spins in diamond. To fill this gap, we are presenting here the results of the simulation of full tensors J_{KL} ($K, L = X, Y, Z$) and describing the J -couplings of nuclear spins ^{13}C in small H-terminated diamond clusters, as well as in a cluster hosting the NV-color center.

2. Methods and Materials

In principle, theoretical foundations of J -coupling are well established [11–14] and there has been considerable progress in calculating the J -coupling characteristics for many simple molecules (e.g., see [12,15–17]) including ^{13}C – ^{13}C pairs [12,16–19]. However, most software packages were previously limited by calculation of the scalar J -coupling constants. Only recently has it become possible to calculate full J -coupling tensors. Here we have used for the purpose the latest version 5.0.2 of the ORCA package. To model a diamond crystal, we used H-terminated carbon clusters. First, in order to test the opportunities of the package, we calculated the J -tensors for all possible pairs ^{13}C – ^{13}C in the diamond-like adamantane molecule $\text{C}_{10}\text{H}_{16}$ (see Figure 1a), for which the isotropic J -coupling constant $^1J_{iso}$ for N–N nuclear spins ^{13}C was experimentally measured to be 31.4 ± 0.5 Hz [20]. Having obtained the value of ~ 29.9 Hz for them (see Figure 2a, below), which was quite close to the above experimental one, we performed similar calculations for the H-terminated carbon cluster $\text{C}_{35}\text{H}_{36}$ (Figure 1b), as well as for the similar cluster $\text{C}_{33}[\text{NV}^-]\text{H}_{36}$ hosting the NV color center (Figure 1c). It should be noted that the choice of such small clusters was due to the fact that, as is known [14–16], the calculations of the J -coupling characteristics are very computationally demanding for even modest-sized molecules. We optimized the cluster geometry using the ORCA 5.0.2 software package with the B3LYP/def2/J/RIJCOSX level of theory and then simulated the n -bond J -coupling tensors $^nJ_{KL}(\text{Ci}, \text{Cj})$ for all possible ^{13}C – ^{13}C pairs in the clusters using the B3LYP/TZVPP/AUTOAUX/decontract level of theory. The functional B3LYP in combination with TZVPP basis is recommended for NMR calculations by ORCA [21,22]. The last two keywords provide a general-purpose auxiliary basis for simultaneously fitting Coulomb, exchange and correlation calculations as well as calculations of integrals for Fermi-contact interaction which require very tight s -functions. Both of them are needed for correct calculations of all contributions to the J -coupling tensor. The package returns matrices describing the diamagnetic, paramagnetic, Fermi-contact, spin-dipolar and spin-dipolar/Fermi contact cross-term contributions to the total $^nJ_{KL}$ tensor in the coordinate systems indicated in Figure 1. Using them and taking into account the known coordinates of carbon atoms belonging to some definite ^{13}C – ^{13}C pair in the cluster, one can find respective J -coupling matrices in the other coordinate system. In particular, for neighboring nuclear spins ^{13}C , separated by a single bond in diamond (~ 1.54 Å), the total $^1J_{KL}$ matrix becomes diagonal with $J_{XX} \approx J_{YY}$ in the coordinate system in which the Z -axis is directed along this bond [9]. In this case it is conventional to describe an axial J -coupling tensor in terms of two parameters: the scalar constant $^1J_{iso}$ and the asymmetric part Δ^1J . Since the magnitude of the J -coupling decreases rapidly with bond order, we will mainly consider here only N–N nuclear spins.

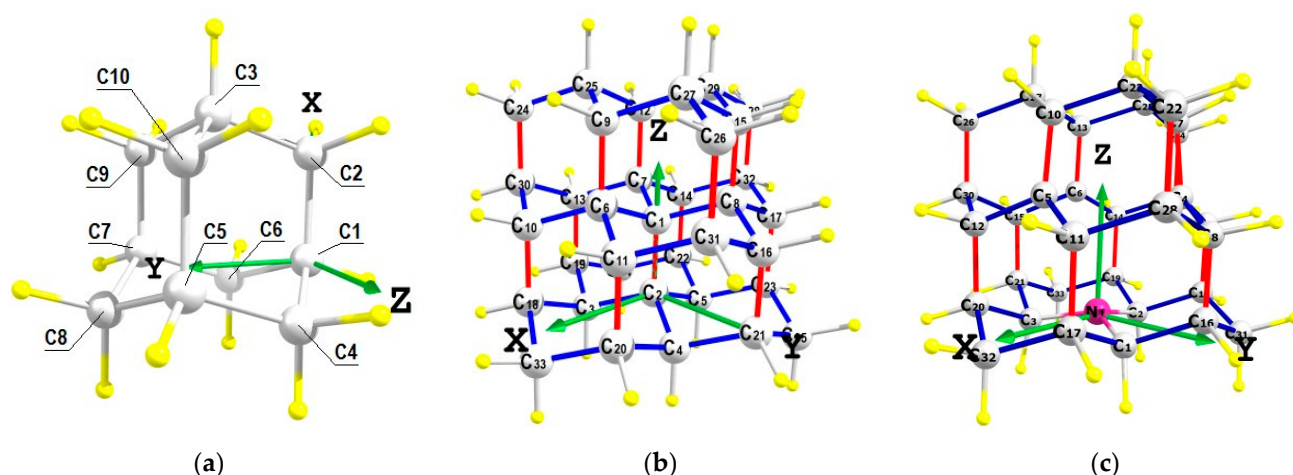


Figure 1. Simulated clusters with the carbon atoms numerated and the coordinate systems indicated. (a) Adamantane molecule $C_{10}H_{16}$; (b) Cluster $C_{35}H_{36}$; (c) Cluster $C_{33}[NV^-]H_{36}$. Carbon atoms are shown in grey; passivating H-atoms in yellow; nitrogen atom N in (c) in purple.

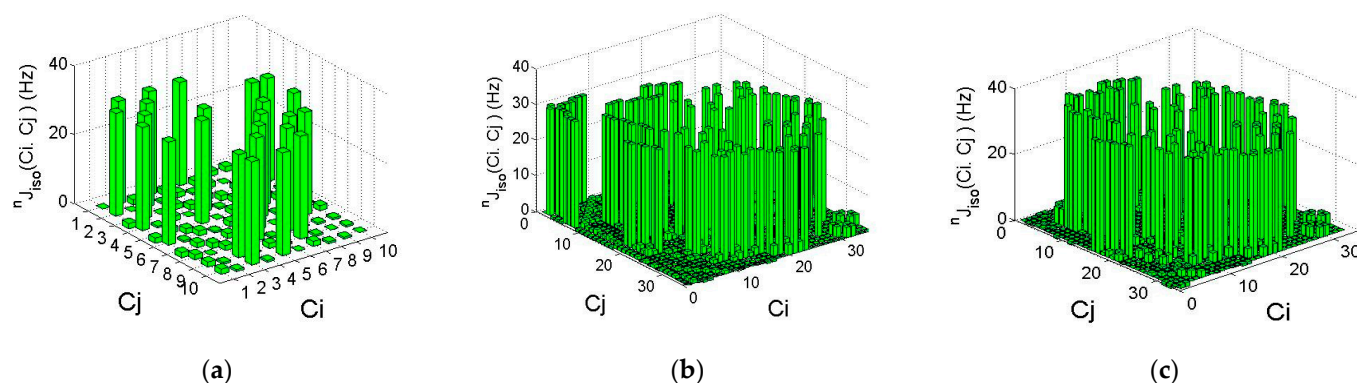


Figure 2. Isotropic scalar constants $nJ_{iso}(Ci, Cj)$ for all possible $^{13}Ci-^{13}Cj$ pairs in (a) adamantane molecule; (b) Cluster $C_{35}H_{36}$; (c) Cluster $C_{33}[NV^-]H_{36}$.

3. Results and Discussion

In the case of adamantane, we first calculated the isotropic J -coupling constants nJ_{iso} for all possible pairs $Ci-Cj$ with the numbers i and j shown in Figure 1a. The simulation was performed in the arbitrarily chosen coordinate system, in which the origin was on the $C1$ atom, the X axis was directed from the $C1$ atom to the $C2$ atom and the Y and Z axes were directed as it is shown in Figure 1a. The results of calculations are illustrated graphically in Figure 2a, which shows, in the form of a bar graph, the calculated values of the isotropic constants $nJ_{iso}(Ci, Cj)$ for pairs of ^{13}C nuclear spins with numbers Ci and Cj , indicated in Figure 1a. In the molecule there are 12 pairs ($C1-C2$, $C1-C4$, $C1-C6$, $C2-C3$, $C3-C9$, $C3-C10$, $C4-C5$, $C5-C8$, $C5-C10$, $C6-C7$, $C7-C8$, $C7-C9$) wherein carbon atoms are nearest-neighbors separated by single $C-C$ bond. For these one-bond pairs, the values of the $^1J_{iso}$ constants were in the range of 29.8–29.92 Hz, i.e., were close to the experimentally measured [20] value of 31.4 ± 0.5 Hz. For all these pairs, the calculated total matrices $^1J_{KL}(Ci, Cj)$ were close to diagonal, since the isotropic Fermi-contact interaction made the main contribution to them. Moreover, taking into account the symmetry of the $N-N$ $Ci-Cj$ pairs about their midpoint in the transformed coordinate system, in which the Z axis is directed along some $Ci-Cj$ bond, it is possible to transform the J -coupling matrices to their simplest diagonal form [9]. As an example, we considered here the $C1-C2$ pair, in which both nuclear spins are located on the X axis (see Figure 1a) so that the transformation of the calculated matrices to the new coordinate system, where the Z axis is directed along the $C1-C2$ bond, is carried out simply by rotation counterclockwise by 90° around the Y

axis. For the C1–C2 pair, the partial matrices in the thus transformed coordinate system are presented below in Table 1.

Table 1. The total J -coupling matrix ${}^1J_{KL}(C1,C2)$ and partial contributions to it (in Hz) for the ${}^{13}C1$ – ${}^{13}C2$ pair in the adamantane molecule calculated in the transformed coordinate system, having the Z axis along the C1–C2 bond.

Diamagnetic contribution:			Paramagnetic contribution:			Fermi-Contact contribution:		
[−0.80	0	0.00	[0.21	0	0.00	[28.91	0	0
0	−0.85	0.08	0	−0.08	−0.03	0	28.91	0
0.00	−0.06	2.53];	0.00	0.04	−1.81];	0	0	28.91];
Spin-Dipolar contribution:			SD/FC cross-term contribution:			Total coupling tensor:		
[0.54	0	0.00	[5.01	0	−0.00	[33.87	0	−0.00
0	0.59	−0.07	0	4.98	−0.06	0	33.55	−0.08
0.00	0.08	2.34];	−0.00	−0.06	−9.99];	−0.00	0.01	21.97]

One can see from these data the relative contributions of various interactions. They also show that the total matrix ${}^1J(C1,C2)$ is, as expected [9], near-diagonal with ${}^1J_{XX}(C1,C2) \approx {}^1J_{YY}(C1,C2)$ so that for this pair the asymmetric part of the J -coupling tensor is $\Delta^1J = {}^1J_{ZZ} - ({}^1J_{XX} + {}^1J_{YY})/2 = -11.74$ Hz. Similar data can be obtained for other pairs of N–N nuclear spins in the adamantane molecule. Figure 2a also shows that the isotropic constants ${}^2J_{iso}$ and ${}^3J_{iso}$ for more distant nuclear spins are only few hertz or less.

The results of similar calculations of isotropic constants ${}^nJ_{iso}$, performed for all possible pairs ${}^{13}C$ – ${}^{13}C$ in the clusters $C_{35}H_{36}$ and $C_{33}[NV^-]H_{36}$, are illustrated by bar graphs shown in Figure 2b,c, respectively. As one can see from Figure 1b, in the case of the cluster $C_{35}H_{36}$ we choose the coordinate systems in which the origin was taken at the C_2 carbon atom and the Z axis was directed from the C_2 to the C_1 atom. In this cluster, there are 595 different ${}^{13}C$ – ${}^{13}C$ pairs with 52 of them being N–N carbons. Among these N–N pairs, 13 have their bonds near-parallel to the chosen Z axis. These bonds are shown in red in Figure 1b. For the remaining 39 N–N pairs, shown in blue in Figure 1b, the angles between their bonds and the Z axis were approximately equal to the tetrahedral angle 109.47° (or $180^\circ - 109.47^\circ$). Respectively, in the case of the cluster $C_{33}[NV^-]H_{36}$, the origin of the coordinate system was taken on the N atom of the NV center and the Z axis coincided with the NV center axis. In this cluster, there are 45 N–N ${}^{13}C$ – ${}^{13}C$ pairs, 12 of them having bonds directed near-parallel to the Z axis. Again, these 12 pairs are shown in red in Figure 1c and the other ones are shown in blue. As one can see from Figure 2b, for the cluster $C_{35}H_{36}$, simulated one-bond constants ${}^1J_{iso}$ were in the range of 29.8–30.0 Hz (for specific values see Table 2), i.e., very close to those obtained for the adamantane molecule. Conversely, in case of the cluster $C_{33}[NV^-]H_{36}$ containing the NV center, there were several pairs of N–N ${}^{13}C$ atoms, located near the vacancy of the NV center, for which the values of the ${}^1J_{iso}$ constants were slightly higher (~ 37.1 Hz) than for the other pairs (~ 31.5 – 31.8 Hz, see Table 2).

The above data on the isotropic constants ${}^1J_{iso}$ for the clusters $C_{35}H_{36}$ and $C_{33}[NV^-]H_{36}$ have been obtained from total J -coupling matrices ${}^1J_{KL}$ calculated for these clusters. Generally, as in the case of adamantane, the matrices have diagonal elements which are much larger than the non-diagonal ones. These diagonal elements are shown in Figure 3a–f for the clusters $C_{35}H_{36}$ and $C_{33}[NV^-]H_{36}$, respectively. In these Figures, the red bars give the values of the corresponding diagonal elements for those adjacent carbon pairs for which the C–C bond is directed almost parallel to the Z axis of the coordinate system used; whereas the blue bars are for pairs for which the C–C bond makes a tetrahedral angle with the Z axis. More specifically, the values of the diagonal elements ${}^1J_{KK}$ ($K = X, Y, Z$) of the J -coupling matrices of N–N ${}^{13}C$ – ${}^{13}C$ pairs shown in red in Figure 3 are given below in Table 2 along with the corresponding values of the isotropic constants shown in Figure 2b,c.

Table 2. Diagonal elements ${}^1J_{KK}(\text{Ci,Cj})$ of total J -coupling tensors (in Hz) and corresponding values of the isotropic constants ${}^1J_{\text{iso}}$ calculated for N–N ${}^{13}\text{Ci}$ – ${}^{13}\text{Cj}$ pairs with their bonds near-parallel to the Z-axis of the coordinate systems shown in Figure 1b,c. The left panel shows the data for the cluster $\text{C}_{35}\text{H}_{36}$; the right panel for the cluster $\text{C}_{33}[\text{NV}^-]\text{H}_{36}$. Atoms C4, C5 and C6 shown in bold in the right panel are the nearest neighbors of the vacancy of the NV center in the cluster $\text{C}_{33}[\text{NV}^-]\text{H}_{36}$.

Cluster $\text{C}_{35}\text{H}_{36}$					Cluster $\text{C}_{33}[\text{NV}^-]\text{H}_{36}$				
Pair Ci,Cj	${}^1J_{xx}$	${}^1J_{yy}$	${}^1J_{zz}$	${}^1J_{\text{iso}}$	Pair Ci,Cj	${}^1J_{xx}$	${}^1J_{yy}$	${}^1J_{zz}$	${}^1J_{\text{iso}}$
C2,C1	33.45	33.45	22.41	29.77	C4,C7	39.93	41.41	30.08	37.14
C6,C9	33.66	33.44	22.52	29.87	C5,C10	42.06	39.12	30.01	37.06
C7,C12	33.49	33.60	22.51	29.87	C6,C13	39.93	41.41	30.08	37.14
C8,C15	33.49	33.60	22.51	29.87	C8,C16	35.88	35.50	23.99	31.79
C18,C10	32.71	32.79	21.56	29.02	C11,C17	35.68	35.71	24.02	31.80
C20,C11	32.71	32.79	21.57	29.02	C9,C18	35.53	35.89	24.00	31.81
C19,C13	32.86	32.67	21.58	29.04	C14,C19	35.53	35.89	24.00	31.81
C22,C14	32.71	32.82	21.58	29.04	C12,C20	35.68	35.71	24.02	31.80
C21,C16	32.85	32.66	21.57	29.03	C15,C21	35.88	35.50	23.99	31.79
C23,C17	32.71	32.82	21.58	29.03	C22,C28	35.41	35.18	23.79	31.46
C30,C24	32.44	32.32	20.90	28.55	C24,C29	35.07	35.53	23.80	31.47
C31,C26	32.44	32.31	20.90	28.55	C26,C30	35.40	35.18	23.79	31.46
C32,C28	32.25	32.51	20.91	28.56					

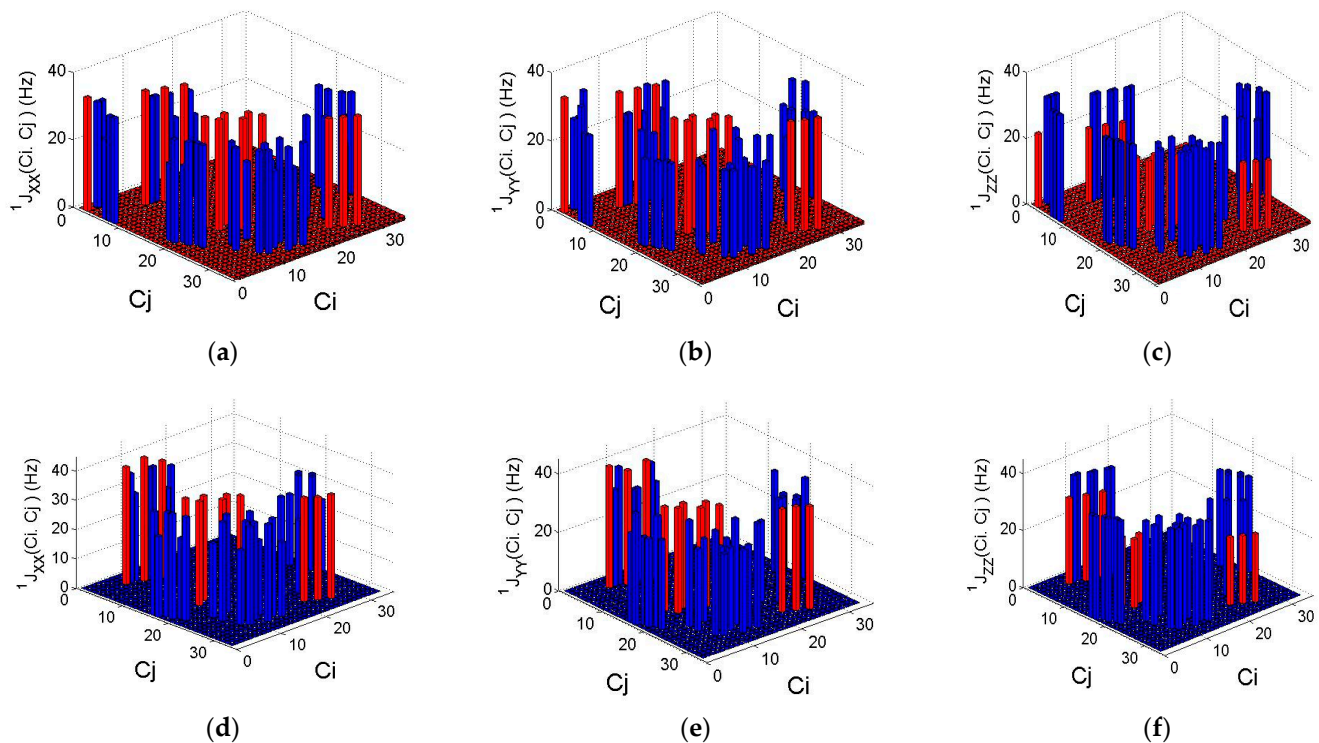


Figure 3. Diagonal elements ${}^1J_{xx}(\text{Ci,Cj})$ (a,d); ${}^1J_{yy}(\text{Ci,Cj})$ (b,e); and ${}^1J_{zz}(\text{Ci,Cj})$ (c,f) of the 1J -coupling matrices, calculated for nearest-neighbor ${}^{13}\text{C}$ – ${}^{13}\text{C}$ pairs in the $\text{C}_{35}\text{H}_{36}$ cluster (Figure 3a,c) and in the $\text{C}_{33}[\text{NV}^-]\text{H}_{36}$ cluster (d–f).

One can see from Figure 3 and, more specifically, from Table 2 that for the Ci–Cj pairs which are near-parallel to the Z axis the values ${}^1J_{xx}(\text{Ci,Cj}) \approx {}^1J_{yy}(\text{Ci,Cj})$ are about one and

a half times larger than $^1J_{ZZ}(\text{Ci,Cj})$. Moreover, the presence of the negatively charged NV[−] center in the cluster C₃₃[NV[−]]H₃₆, which introduces additional electron density, leads to some increase in the diagonal elements $^1J_{KK}$ of the J -coupling matrices for all Ci–Cj pairs compared with the cluster C₃₅H₃₆. As follows from Table 2, such an increase in the $^1J_{KK}$ values is especially pronounced (~9%) for the C4,C7; C5,C10 and C6,C13 pairs, in which the atoms C4, C5 and C6 are the nearest neighbors of the vacancy of the NV center on which the electron density of the center is mainly localized [23]. A similar increase in J -coupling takes place for other pairs C4/5/6–Cj, for which the corresponding bonds make an angle of ~109.47° with the axis Z of the selected coordinate system.

4. Conclusions

For the first time, the total tensors describing the indirect interaction of ¹³C nuclear spins in adamantane molecule, H-terminated diamond cluster C₃₅H₃₆ and in the cluster C₃₃[NV[−]]H₃₆ hosting NV centers have been calculated by quantum chemistry methods. It is shown that the presence of the NV center leads to a change in characteristics of the indirect interaction of ¹³C nuclear spins. The results obtained are important for quantum information and sensor applications, in particular, for the creation of long-lived quantum memory based on singlet-state ¹³C–¹³C dimers in diamond [3], creation of nanoscale NV-based quantum sensors that ensure the detection of adsorbed molecules/radicals on the surface of nanostructured diamond [4] and the determination of their chemical structure. Such sensors can be used to study biological processes at the level of individual cells, membranes, nerve fibers, targeted drug delivery and control of such delivery. The data obtained can also be useful for studies of NMR in the zero-to ultralow-field regime [24–27], where the internal spin interactions are dominated in their natural environment. An analysis of the dynamics of multi-spin systems ¹⁴NV–¹³C–¹³C with the account of both direct dipole–dipole interactions of ¹³C nuclear spins and of their J -coupling, as well as modeling of the NMR spectra of such objects, will be presented elsewhere.

Author Contributions: Conceptualization, A.N. and A.P.; methodology, A.N., A.P. and S.K. (Semen Kuten); software, A.P., D.M. and D.L.; validation, N.K. and S.K. (Sergei Kilin); formal analysis, A.N.; investigation, A.N., A.P. and S.K. (Semen Kuten); resources, D.M. and D.L.; data curation, A.P. and S.K. (Semen Kuten); writing—original draft preparation, A.N.; writing—review and editing, A.N.; visualization, A.N. and N.K.; supervision, N.K. and S.K. (Sergei Kilin); project administration, A.N. and N.K.; funding acquisition, A.N. and N.K. All authors have read and agreed to the published version of the manuscript.

Funding: This research was funded by RSF, project No. 21-42-04416, and, in the part of calculations for adamantane, by the Belarus State Scientific Program Convergence-2025.

Institutional Review Board Statement: This study did not require ethical approval.

Informed Consent Statement: Not applicable.

Data Availability Statement: Not applicable.

Acknowledgments: All Orca 5.0.2 package computations were performed on KAUST's Ibex HPC. The authors thank the KAUST Supercomputing Core Lab team for assistance with execution tasks on Skylake nodes. We are also grateful to F. Jelezko for very useful cooperation.

Conflicts of Interest: The authors declare no conflict of interest.

References

1. Schwartz, I.; Rosskopf, J.; Schmitt, S.; Tratzmiller, B.; Chen, Q.; McGuinness, L.P.; Jelezko, F.; Plenio, M.B. Blueprint for nanoscale NMR. *Sci. Rep.* **2019**, *9*, 6938. [[CrossRef](#)] [[PubMed](#)]
2. Barry, J.F.; Schloss, J.M.; Bauch, E.; Turner, M.J.; Hart, C.A.; Pham, L.M.; Walsworth, R.L. Sensitivity optimization for NV-diamond magnetometry. *Rev. Mod. Phys.* **2020**, *92*, 015004. [[CrossRef](#)]
3. Chen, Q.; Schwarz, I.; Plenio, M.B. Steady-state preparation of long-lived nuclear spin singlet pairs at room temperature. *Phys. Rev. B* **2017**, *95*, 224105. [[CrossRef](#)]

4. Glenn, D.R.; Bucher, D.B.; Lee, J.; Lukin, M.D.; Park, H.; Walsworth, R.L. High-resolution magnetic resonance spectroscopy using a solid-state spin sensor. *Nature* **2018**, *95*, 55535. [[CrossRef](#)]
5. Harris, K.J.; Bryce, D.L.; Wasylishen, R.E. NMR line shapes from AB spin systems in solids—The role of antisymmetric spin-spin coupling. *Can. J. Chem.* **2009**, *87*, 1338–1351. [[CrossRef](#)]
6. Frydman, L. Spin-1/2 and beyond: A perspective in solid state NMR spectroscopy. *Annu. Rev. Phys. Chem.* **2001**, *52*, 463–498. [[CrossRef](#)]
7. Reif, B.; Ashbrook, S.E.; Emsley, L.; Hong, M. Solid-state NMR spectroscopy. *Nat. Rev. Methods Primers* **2021**, *1*, 2. [[CrossRef](#)]
8. Vaara, J.; Jokisaari, J.; Wasylishen, R.E.; Bryce, D.L. Spin-spin coupling tensors as determined by experiment and computational chemistry. *Prog. Nucl. Magn. Reson. Spectrosc.* **2002**, *41*, 233–304. [[CrossRef](#)]
9. Christensen, B.; Price, J.C. NMR lineshape of ^{29}Si in single-crystal silicon. *Phys. Rev. B* **2017**, *95*, 134417. [[CrossRef](#)]
10. Lefmann, K.; Buras, B.; Pedersen, E.J.; Shabanova, E.S.; Thorsen, P.A.; Rasmussen, F.B.; Sellschop, J.P.F. NMR spectra of pure ^{13}C diamond. *Phys. Rev B* **1994**, *50*, 15623–15627. [[CrossRef](#)]
11. Ramsey, F. Electron Coupled Interactions between Nuclear Spins in Molecules. *Phys. Rev.* **1953**, *91*, 303–307. [[CrossRef](#)]
12. Wray, V. Carbon-carbon coupling constants: A compilation of data and a practical guide. *Prog. NMR Spectrosc.* **1979**, *13*, 177–256. [[CrossRef](#)]
13. Helgaker, T.; Jaszunski, M.; Ruud, K. Ab Initio Methods for the Calculation of NMR Shielding and Indirect Spin–Spin Coupling Constants. *Chem. Rev.* **1999**, *99*, 293–352. [[CrossRef](#)]
14. Helgaker, T.; Jaszunski, M.; Pecul, M. The quantum-chemical calculation of NMR indirect spin–spin coupling constants. *Prog. Nucl. Magn. Reson. Spectrosc.* **2008**, *53*, 249–268. [[CrossRef](#)]
15. Antušek, A.; Kędziera, D.; Jackowski, K.; Jaszunski, M.; Makulski, W. Indirect spin–spin coupling constants in CH_4 , SiH_4 and GeH_4 —Gas-phase NMR experiment and ab initio calculations. *Chem. Phys.* **2008**, *352*, 320–326. [[CrossRef](#)]
16. Krivdin, L.B.; Contreras, R.H. Recent Advances in Theoretical Calculations of Indirect Spin–Spin Coupling Constants. *Annu. Rep. Nucl. Magn. Reson. Spectrosc.* **2007**, *61*, 133–245.
17. Kamienska-Trela, K. One-bond ^{13}C – ^{13}C Spin-Spin Coupling Constants. *Annu. Rep. NMR Spectrosc.* **1995**, *30*, 131–222.
18. Jaszunski, M.; Ruud, R.; Helgaker, T. Density-functional theory calculation of the nuclear magnetic resonance indirect nuclear spin–spin coupling constants in C_{60} . *Mol. Phys.* **2003**, *101*, 1997–2002. [[CrossRef](#)]
19. Peralta, J.E.; Barone, V.; Scuseria, G.E.; Contrera, R.H. Density Functional Theory Calculation of Indirect Nuclear Magnetic Resonance Spin-Spin Coupling Constants in C_{70} . *J. Am. Chem. Soc.* **2004**, *126*, 7428–7429. [[CrossRef](#)]
20. Gay, I.D.; Jones, C.H.W.; Sharma, R.D. INADEQUATE in the Solid State. Homonuclear Couplings in $[(\text{CH}_3)_2\text{SnE}]_3$. *J. Magn. Reson.* **1991**, *91*, 186–189.
21. NMR Spectra. Available online: https://www.orcasoftware.de/tutorials_orca/spec/NMR.html (accessed on 22 April 2022).
22. ORCA Manual Version 5.0.2P.320. Available online: <https://orcaforum.kofo.mpg.de/app.php/dlxt/?cat=18> (accessed on 22 April 2022).
23. Nizovtsev, A.P.; Kilin, S.Y.; Pushkarchuk, A.L.; Pushkarchuk, V.A.; Kuten, S.A.; Zhikol, O.A.; Schmitt, S.; Uden, T.; Jelezko, F. Non-flipping ^{13}C spins near an NV center in diamond: Hyperfine and spatial characteristics by density functional theory simulation of the $\text{C}_{510}[\text{NV}]\text{H}_{252}$ cluster. *New J. Phys.* **2018**, *20*, 023022. [[CrossRef](#)]
24. Theis, T.; Blanchard, J.W.; Butler, M.C.; Ledbetter, M.P.; Budker, D.; Pines, A. Chemical analysis using J-coupling multiplets in zero-field NMR. *Chem. Phys. Lett.* **2013**, *580*, 160–165. [[CrossRef](#)]
25. Blanchard, J.W.; Budker, D. Zero- to Ultralow-field NMR. *eMagRes* **2016**, *5*, 1395–1410.
26. Jiang, M.; Wu, T.; Blanchard, J.W.; Feng, G.; Peng, X.; Budker, D. Experimental benchmarking of quantum control in zero-field nuclear magnetic resonance. *Sci. Adv.* **2018**, *4*, eaar6327. [[CrossRef](#)] [[PubMed](#)]
27. DeVience, S.J.; Greer, M.; Mandal, S.; Rosen, M.S. Homonuclear J-Coupling Spectroscopy at Low Magnetic Fields using Spin-Lock Induced Crossing. *ChemPhysChem* **2021**, *22*, 2128–2137. [[CrossRef](#)] [[PubMed](#)]